Enhancing AFM Image Analysis and Prediction through Machine Learning and Style Translation

Jie Huang
jie.huang@aalto.fi

Surfaces and Interfaces at the Nanoscale (SIN)
Department of Applied Physics, School of Science, Aalto University

Surfaces and Interfaces at the Nanoscale (SIN)
Aalto University School of Science

Non-Contact Atomic Force Microscopy (NC-AFM)

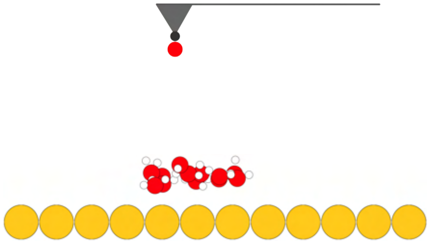

- The cantilever's oscillation is driven by a circuit.
- NC-AFM tip never touches the sample.
- A CO molecule is attached to the tip.

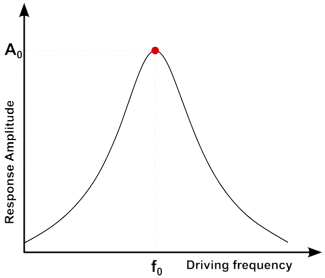

The response curve shows the amplitude of the cantilever (a driven oscillator) at frequencies near its natural frequency f_0.

A feedback loop changes the driving frequency to maintain the maximum oscillating amplitude. The difference $\Delta f = f - f_0$ is recorded for imaging.

Non-Contact Atomic Force Microscopy (NC-AFM)

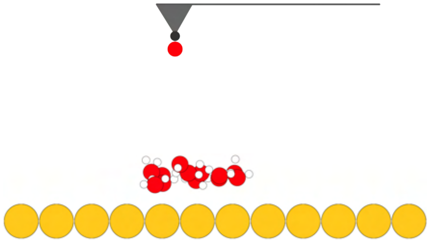

- The cantilever's oscillation is driven by a circuit.
- NC-AFM tip never touches the sample.
- A CO molecule is attached to the tip.

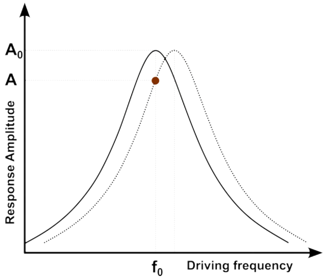

The response curve shows the amplitude of the cantilever (a driven oscillator) at frequencies near its natural frequency f_0.

A feedback loop changes the driving frequency to maintain the maximum oscillating amplitude. The difference $\Delta f = f - f_0$ is recorded for imaging.

Non-Contact Atomic Force Microscopy (NC-AFM)

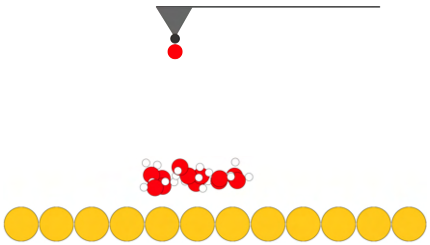

- The cantilever's oscillation is driven by a circuit.
- NC-AFM tip never touches the sample.
- A CO molecule is attached to the tip.

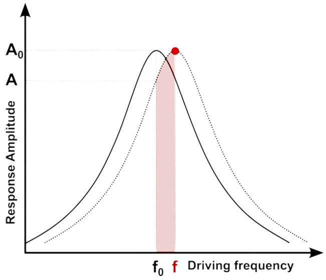

The response curve shows the amplitude of the cantilever (a driven oscillator) at frequencies near its natural frequency f_0.

A feedback loop changes the driving frequency to maintain the maximum oscillating amplitude. The difference $\Delta f = f - f_0$ is recorded for imaging.

AFM Images

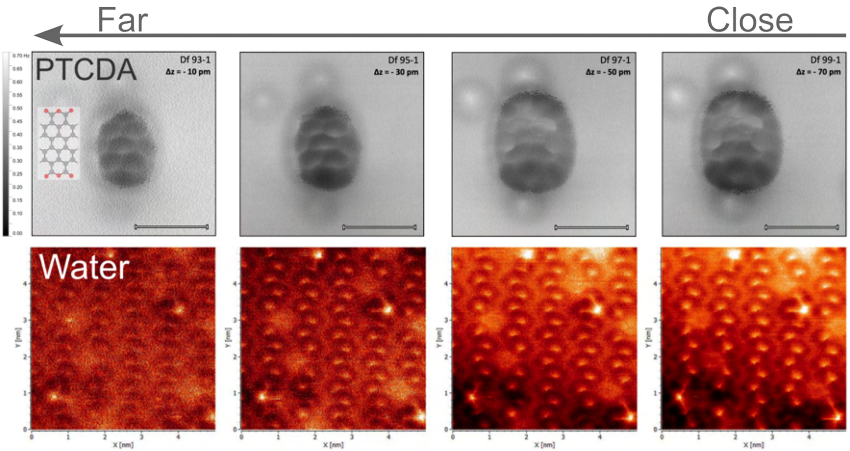

CO tip NC-AFM images of **PTCDA** and **water molecules** on **Calcite(104)** at different heights at T = 5 K[1]

[1] PTCDA and water on Calcite AFM image source: Jonas Heggemann, Paul Laubrock, Tim Dierker and Philipp Rahe, Universität Osnabrück, 2024.

AFM Simulation through Probe Particle Model (PPM)

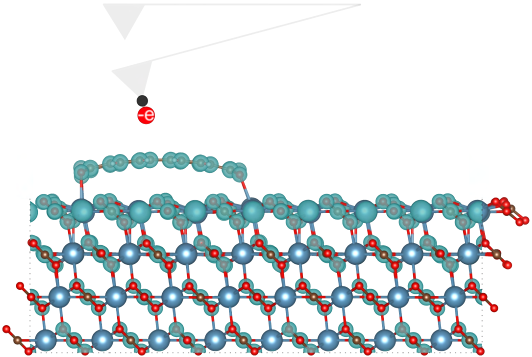

PPM[2,3,4]: Its inputs include the **optimized configuration** and corresponding **electrostatic potential** calculated by Density Functional Theory (DFT); Its output are the **simulation AFM** (**PPAFM**) images at different height.

[2] Hapala, P. et al., *Phys. Rev. B*, 2014, 90(8), 085421. DOI: 10.1103/physrevb.90.085421.

[3] Hapala, P. et al., *Phys. Rev. Lett.*, 2014, 113(22), 226101. DOI: 10.1103/physrevlett.113.226101

[4] Oinonen, N. et al., *Comput. Phys. Commun.*, 2024, 305, 109341. DOI: 10.1016/j.cpc.2024.109341

Manual Structure Discover Workflow

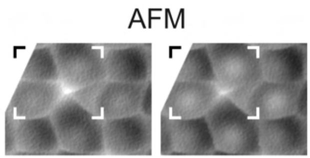

Manual Structure Discover Workflow

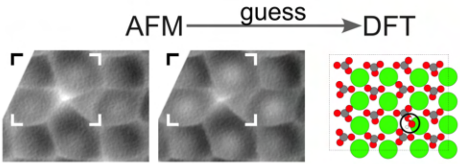

Manual Structure Discover Workflow

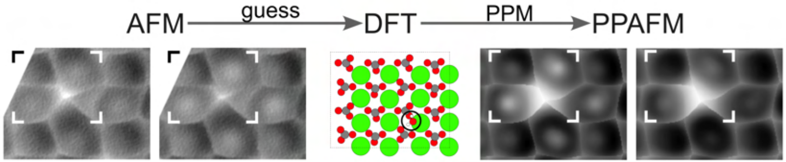

Manual Structure Discover Workflow

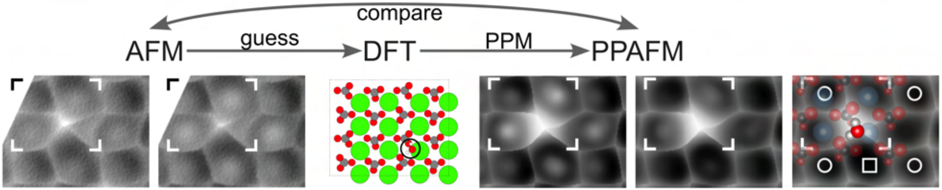

Manual Structure Discover Workflow

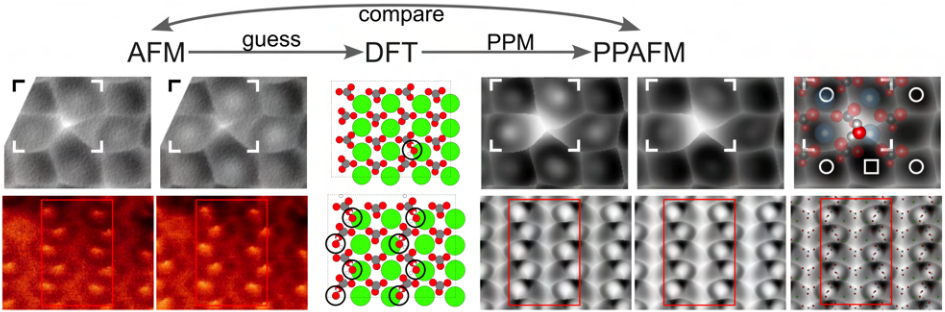

Manual Structure Discover Workflow

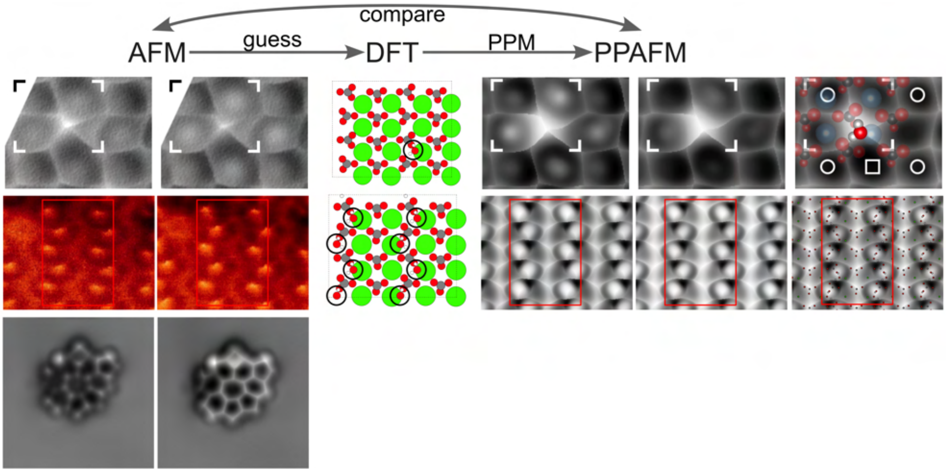

Manual Structure Discover Workflow

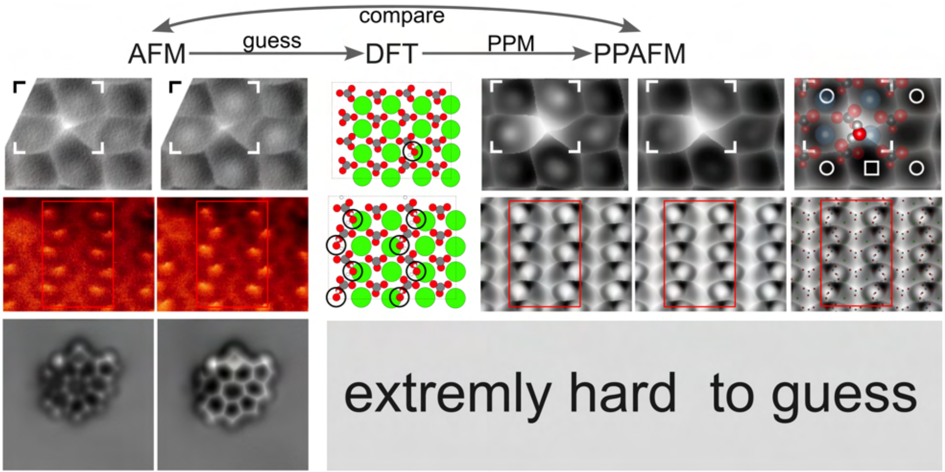

Automatic Structure Discovery Through Machine Learning (ML)

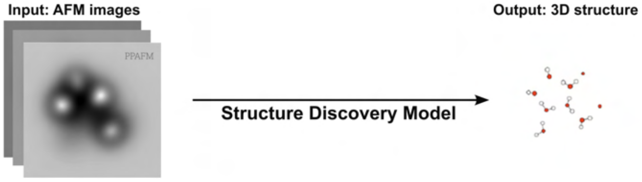

ML models [5,6,7] **trained with simulation datasets**, and **applied on experimental AFM images** to discover 3D structure automatically.

[5] Oinonen, N. et al., *MRS Bulletin*, 2022, 47(9), 895-905. DOI: 10.1557/s43577-022-00324-3.
[6] Kurki, L. et al., *ACS Nano*, 2024, 18(17), 11130-11138. DOI: 10.1021/acsnano.3c12654.
[7] Priante, D. et al., *ACS Nano*, 2024, 18(1), 1234-1245. DOI: 10.1021/acsnano.3c10958

Automatic Structure Discovery Through Machine Learning (ML)

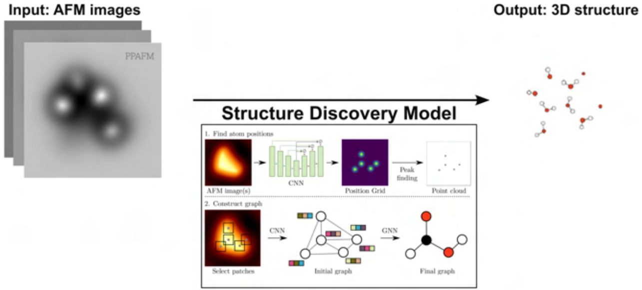

ML models [5,6,7] **trained with simulation datasets**, and **applied on experimental AFM images** to discover 3D structure automatically.

[5] Oinonen, N. et al., *MRS Bulletin*, 2022, 47(9), 895-905. DOI: 10.1557/s43577-022-00324-3.
[6] Kurki, L. et al., *ACS Nano*, 2024, 18(17), 11130-11138. DOI: 10.1021/acsnano.3c12654.
[7] Priante, D. et al., *ACS Nano*, 2024, 18(1), 1234-1245. DOI: 10.1021/acsnano.3c10958

Automatic Structure Discovery Through Machine Learning (ML)

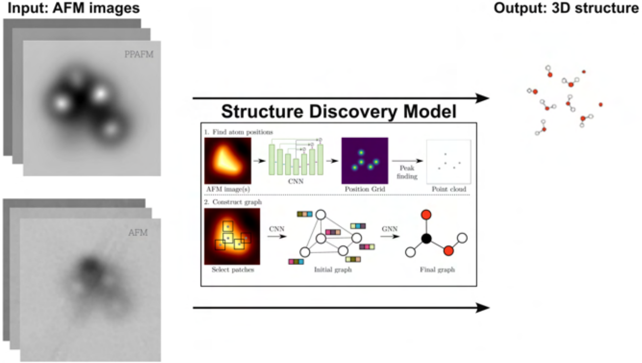

ML models [5,6,7] **trained with simulation datasets**, and **applied on experimental AFM images** to discover 3D structure automatically.

[5] Oinonen, N. et al., *MRS Bulletin*, 2022, 47(9), 895-905. DOI: 10.1557/s43577-022-00324-3.
[6] Kurki, L. et al., *ACS Nano*, 2024, 18(17), 11130-11138. DOI: 10.1021/acsnano.3c12654.
[7] Priante, D. et al., *ACS Nano*, 2024, 18(1), 1234-1245. DOI: 10.1021/acsnano.3c10958

Automatic Structure Discovery Through Machine Learning (ML)

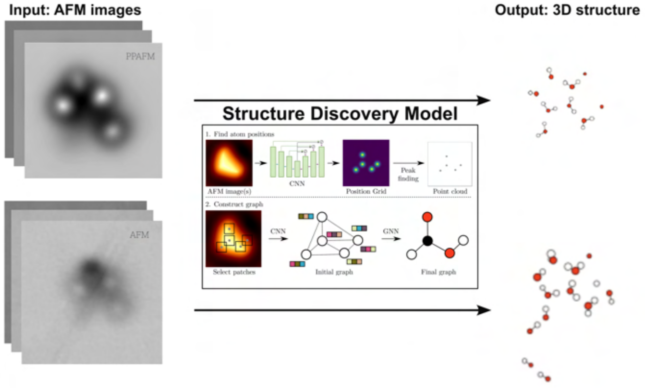

ML models [5,6,7] **trained with simulation datasets**, and **applied on experimental AFM images** to discover 3D structure automatically.

[5] Oinonen, N. et al., *MRS Bulletin*, 2022, 47(9), 895-905. DOI: 10.1557/s43577-022-00324-3.
[6] Kurki, L. et al., *ACS Nano*, 2024, 18(17), 11130-11138. DOI: 10.1021/acsnano.3c12654.
[7] Priante, D. et al., *ACS Nano*, 2024, 18(1), 1234-1245. DOI: 10.1021/acsnano.3c10958

Automatic Structure Discovery Through Machine Learning (ML)

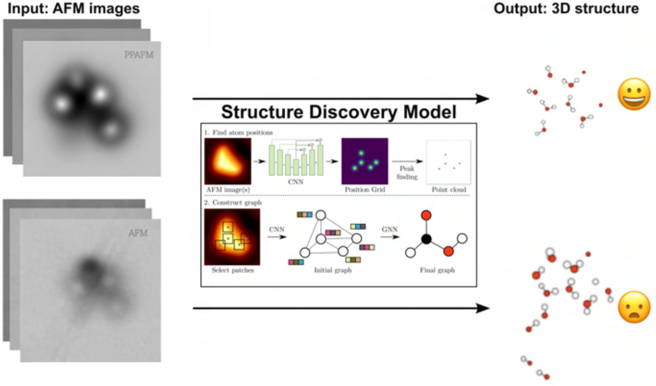

ML models [5,6,7] **trained with simulation datasets**, and **applied on experimental AFM images** to discover 3D structure automatically.

[5] Oinonen, N. et al., *MRS Bulletin*, 2022, 47(9), 895-905. DOI: 10.1557/s43577-022-00324-3.
[6] Kurki, L. et al., *ACS Nano*, 2024, 18(17), 11130-11138. DOI: 10.1021/acsnano.3c12654.
[7] Priante, D. et al., *ACS Nano*, 2024, 18(1), 1234-1245. DOI: 10.1021/acsnano.3c10958

Automatic Structure Discovery Through Machine Learning (ML)

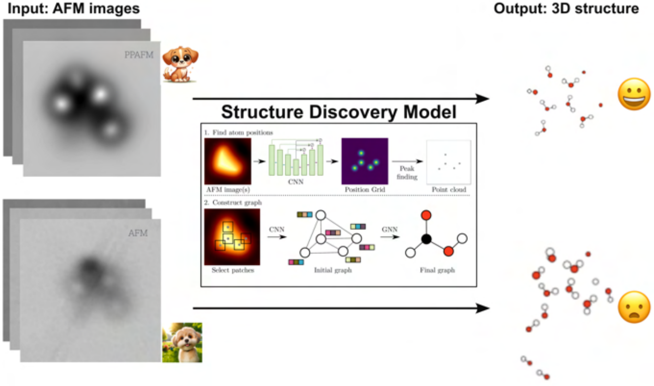

ML models [5,6,7] **trained with simulation datasets**, and **applied on experimental AFM images** to discover 3D structure automatically.

[5] Oinonen, N. et al., *MRS Bulletin*, 2022, 47(9), 895-905. DOI: 10.1557/s43577-022-00324-3.
[6] Kurki, L. et al., *ACS Nano*, 2024, 18(17), 11130-11138. DOI: 10.1021/acsnano.3c12654.
[7] Priante, D. et al., *ACS Nano*, 2024, 18(1), 1234-1245. DOI: 10.1021/acsnano.3c10958

Automatic Structure Discovery Through Machine Learning (ML)

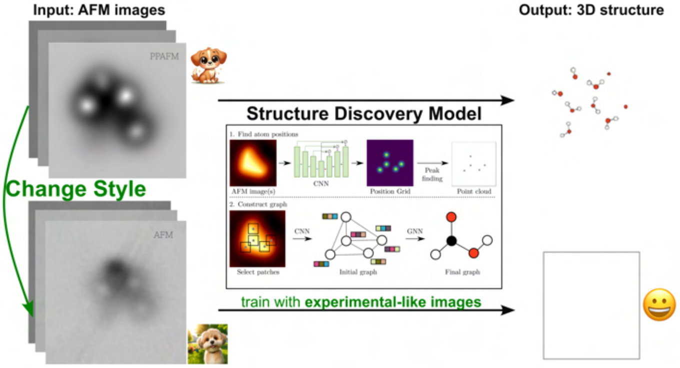

ML models [5,6,7] **trained with simulation datasets**, and **applied on experimental AFM images** to discover 3D structure automatically.

[5] Oinonen, N. et al., *MRS Bulletin*, 2022, 47(9), 895-905. DOI: 10.1557/s43577-022-00324-3.
[6] Kurki, L. et al., *ACS Nano*, 2024, 18(17), 11130-11138. DOI: 10.1021/acsnano.3c12654.
[7] Priante, D. et al., *ACS Nano*, 2024, 18(1), 1234-1245. DOI: 10.1021/acsnano.3c10958

Motivation and Hypothesis

How can we get **better structure predictions** on **experimental AFM images**?

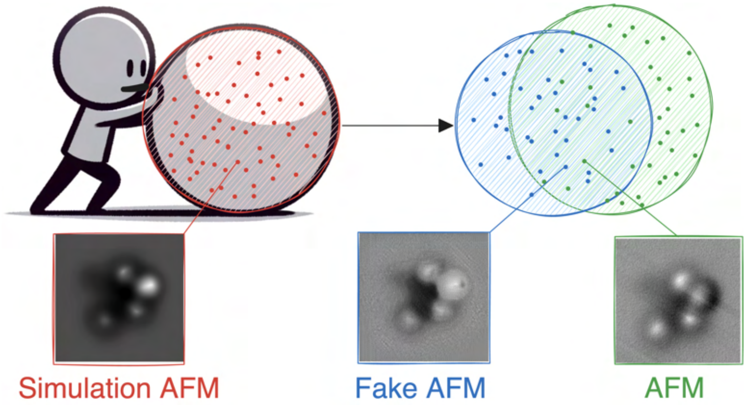

Make simulation AFM images look like real AFM images, and **use these fake AFM images in training** with the expectation that the ML model performance would increase.

Style Translation between Two Domains through CycleGAN

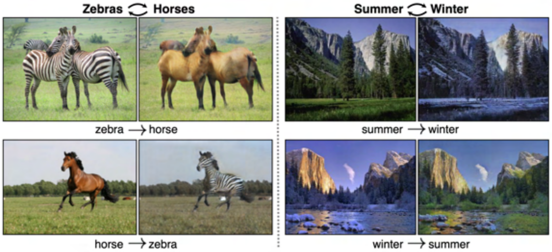

- CycleGAN [8] learns two image-to-image generators to translate image style.
- CycleGAN **learns where to make modifications automatically**.

[8] Zhu, J.-Y. et al., 2020, arXiv:1703.10593.

Style Translation between Two Domains through CycleGAN

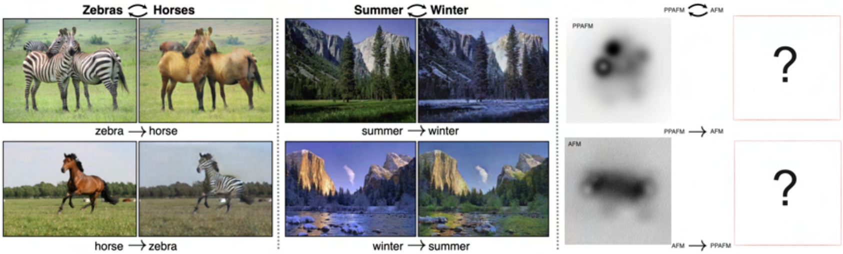

- CycleGAN [8] learns two image-to-image generators to translate image style.
- CycleGAN **learns where to make modifications automatically**.

[8] Zhu, J.-Y. et al., 2020, arXiv:1703.10593.

Style translation between PPAFM and AFM

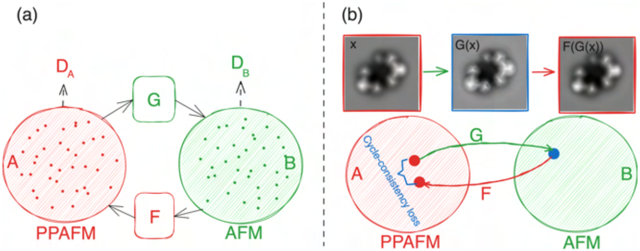

(a) CycleGAN includes two mapping functions G: A $\rightarrow$ B and F: B $\rightarrow$ A, and associated adversarial discriminators D_{A} and D_{B}, which encourages G to translate A into outputs indistinguishable from domain B, and vice versa for D_{A} and F. (b) Cycle consistency ensures that converting from one domain to another and back again returns to the original starting point.

$$\mathcal{L}\left(G, F, D_{\text{A}}, D_{\text{B}}\right) = \mathcal{L}_{\text{GAN}}\left(G, D_{\text{B}}, \text{A}, \text{B}\right) + \mathcal{L}_{\text{GAN}}\left(F, D_{\text{A}}, \text{B}, \text{A}\right) + \lambda \mathcal{L}_{\text{cyc}}(G, F) \tag{1}$$

Style translation between PPAFM and AFM

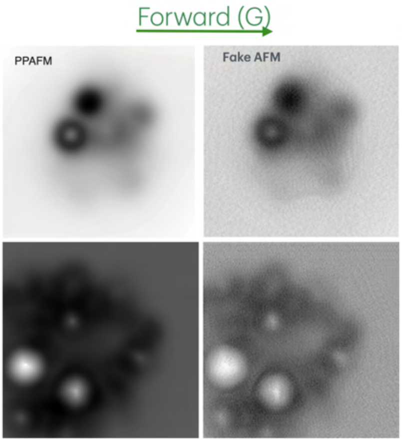

The forward generator **turns PPAFM images into experimental-like AFM images**.

Style translation between PPAFM and AFM

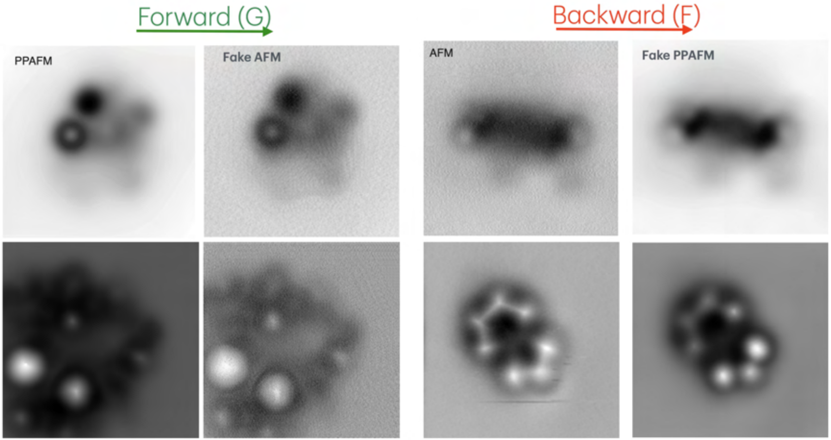

The forward generator **turns PPAFM images into experimental-like AFM images**. The backward generator turns AFM to PPAFM-like images.

Style Translation Evaluation

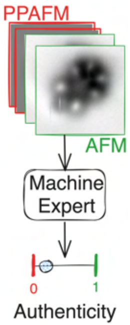

Style translation evaluation from the perspective of **a well trained machine expert**.

Style Translation Evaluation

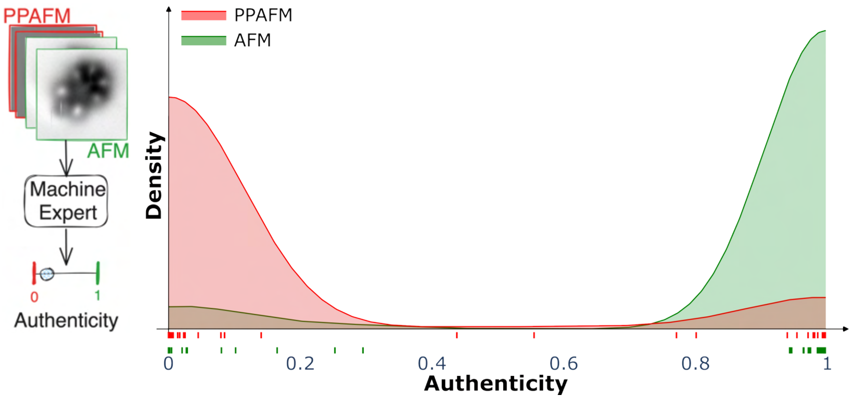

Style translation evaluation from the perspective of **a well trained machine expert**.

Style Translation Evaluation

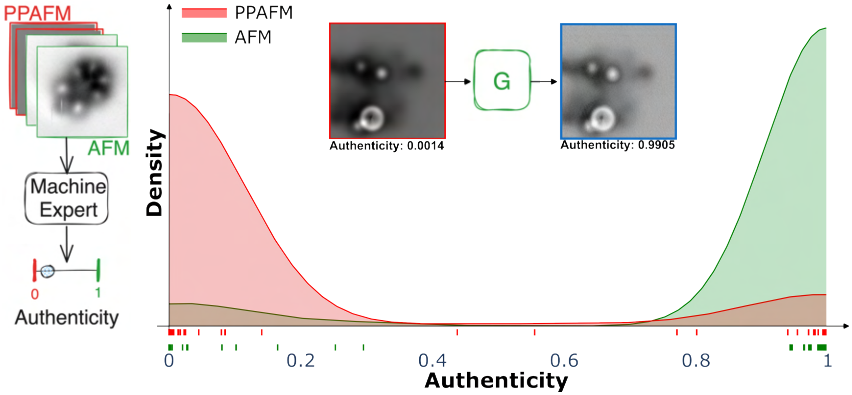

Style translation evaluation from the perspective of **a well trained machine expert**.

Style Translation Evaluation

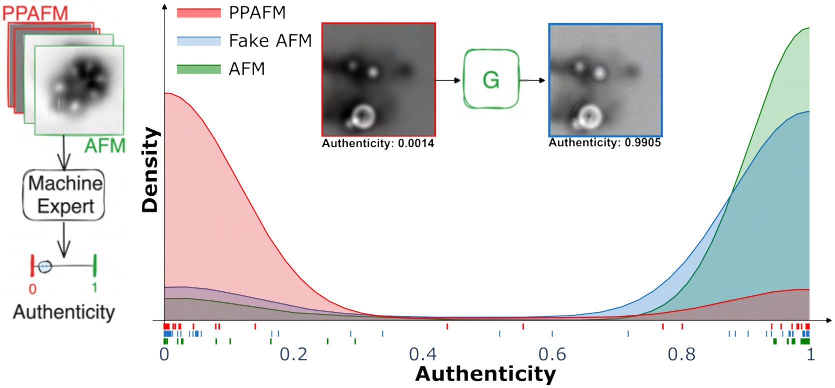

Style translation evaluation from the perspective of **a well trained machine expert**.

Style Translation Evaluation

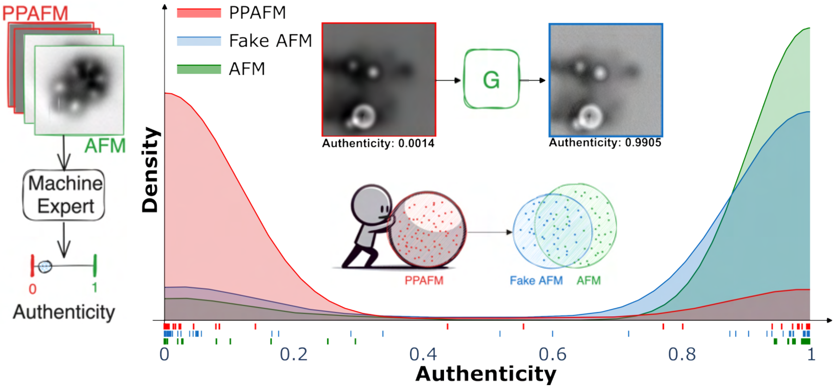

Style translation evaluation from the perspective of **a well trained machine expert**.

Style Translation Evaluation

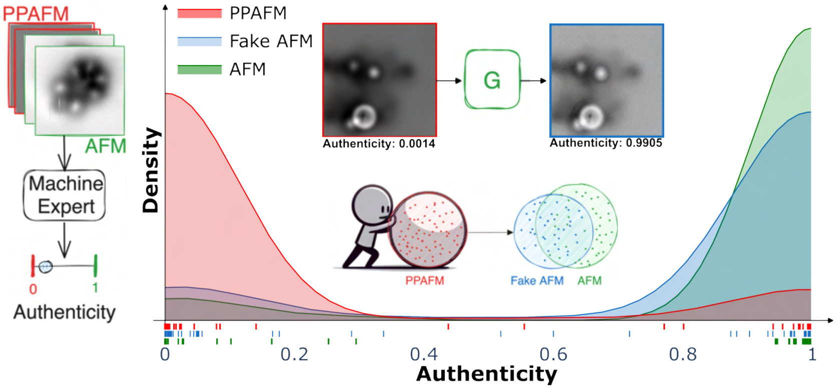

Style translation evaluation from the perspective of **a well trained machine expert**. The trained image-to-image generator shows the ability to **turn simulation distribution to a distribution that is closer to real distribution**.

Training and evaluating the structure discovery

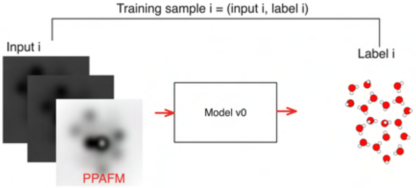

Train models which shares the same network structure **with different datasets**. Then the same experimental AFM images are inputted to these two models.

Training and evaluating the structure discovery

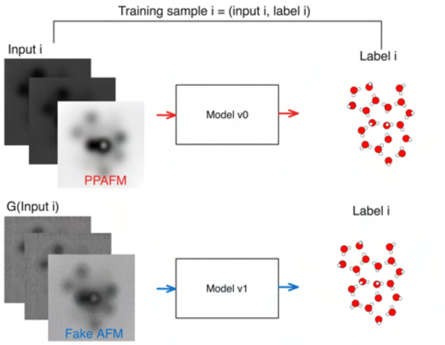

Train models which shares the same network structure **with different datasets**. Then the same experimental AFM images are inputted to these two models.

Training and evaluating the structure discovery

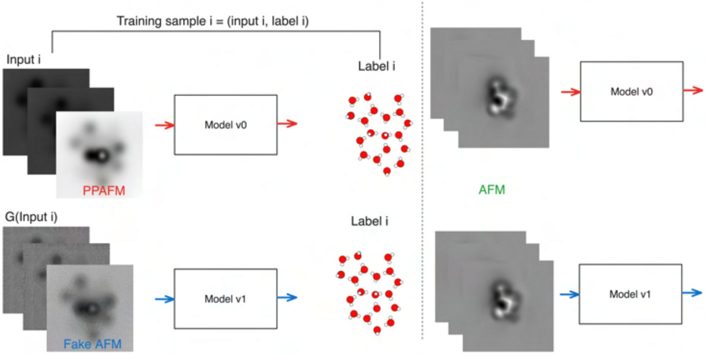

Train models which shares the same network structure **with different datasets**. Then the same experimental AFM images are inputted to these two models.

Training and evaluating the structure discovery

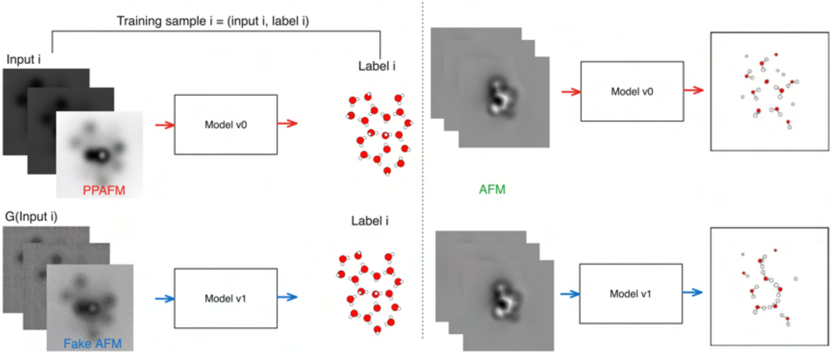

Train models which shares the same network structure **with different datasets**. Then the same experimental AFM images are inputted to these two models.

Structure predictions from model v0 and v1

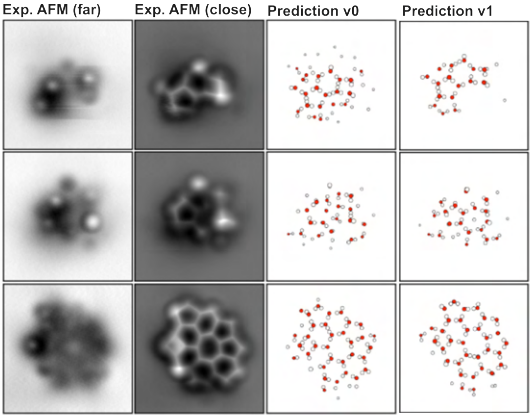

The model trained on the dataset of style-translated fake AFM images seems can handle experiment feature better.

No answer structures for the given AFM images. It's hard to tell which model performs better by directly looking as these predicted structures.

Structure properties

Instead of comparing the individual structure, we compare the structural properties which are calculated through many structures.

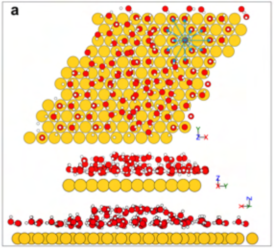

(a) One configuration of water clusters and Au (111) surface. (b, c) **The radial distribution function** (RDF) $g_{\alpha\beta}(r) = \frac{n(r)}{4\pi r^2 \cdot \Delta r \cdot \rho}$ for O-O and O-H pairs; and (d, e) the **angular distribution functions** (ADF) for H-O-H, and O-H-O angles of the relaxed structures used to generate PPAFM.

Structure properties

Instead of comparing the individual structure, we compare the structural properties which are calculated through many structures.

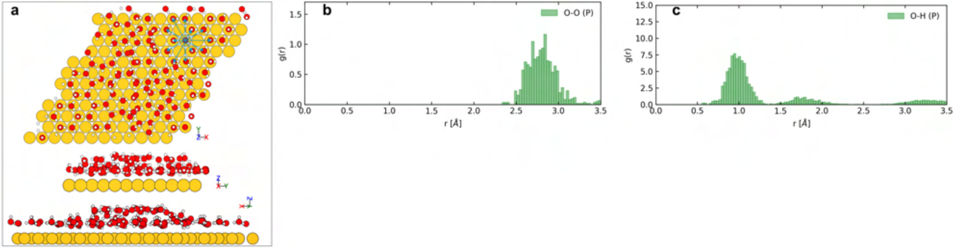

(a) One configuration of water clusters and Au (111) surface. (b, c) **The radial distribution function** (RDF) $g_{\alpha\beta}(r) = \frac{n(r)}{4\pi r^2 \cdot \Delta r \cdot \rho}$ for O-O and O-H pairs; and (d, e) the **angular distribution functions** (ADF) for H-O-H, and O-H-O angles of the relaxed structures used to generate PPAFM.

Structure properties

Instead of comparing the individual structure, we compare the structural properties which are calculated through many structures.

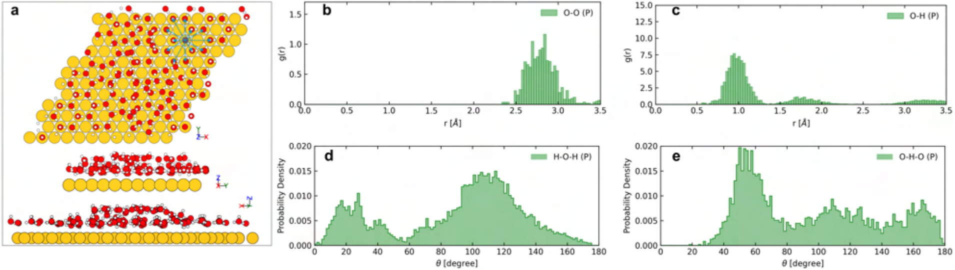

(a) One configuration of water clusters and Au (111) surface. (b, c) **The radial distribution function** (RDF) $g_{\alpha\beta}(r) = \frac{n(r)}{4\pi r^2 \cdot \Delta r \cdot \rho}$ for O-O and O-H pairs; and (d, e) the **angular distribution functions** (ADF) for H-O-H, and O-H-O angles of the relaxed structures used to generate PPAFM.

Prediction evaluations

Performance evaluation on **experimental AFM** images by comparing the **cosine similarity** $S(\mathbf{X}_0, \mathbf{X}_i) = \frac{\mathbf{X}_0 \cdot \mathbf{X}_i}{\|\mathbf{X}_0\| \|\mathbf{X}_i\|}$ between the properties $\mathbf{X}_i$ calculated from predicted structures and the reference values $\mathbf{X}_0$.

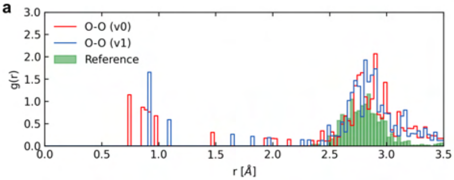

Prediction evaluations

Performance evaluation on **experimental AFM** images by comparing the **cosine similarity** $S(\mathbf{X}_0, \mathbf{X}_i) = \frac{\mathbf{X}_0 \cdot \mathbf{X}_i}{\|\mathbf{X}_0\| \|\mathbf{X}_i\|}$ between the properties $\mathbf{X}_i$ calculated from predicted structures and the reference values $\mathbf{X}_0$.

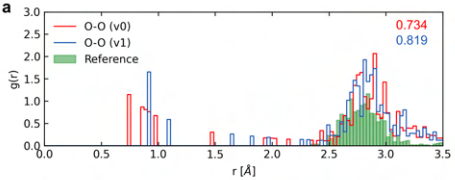

Prediction evaluations

Performance evaluation on **experimental AFM** images by comparing the **cosine similarity** $S(\mathbf{X}_0, \mathbf{X}_i) = \frac{\mathbf{X}_0 \cdot \mathbf{X}_i}{\|\mathbf{X}_0\| \|\mathbf{X}_i\|}$ between the properties $\mathbf{X}_i$ calculated from predicted structures and the reference values $\mathbf{X}_0$.

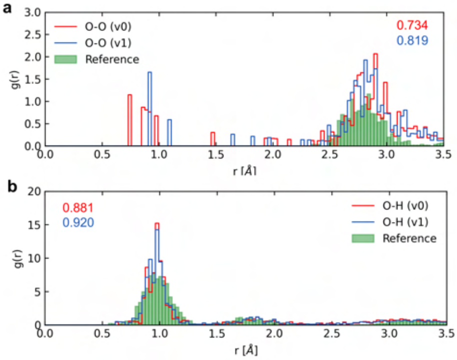

Prediction evaluations

Performance evaluation on **experimental AFM** images by comparing the **cosine similarity** $S(\mathbf{X}_0, \mathbf{X}_i) = \frac{\mathbf{X}_0 \cdot \mathbf{X}_i}{\|\mathbf{X}_0\| \|\mathbf{X}_i\|}$ between the properties $\mathbf{X}_i$ calculated from predicted structures and the reference values $\mathbf{X}_0$.

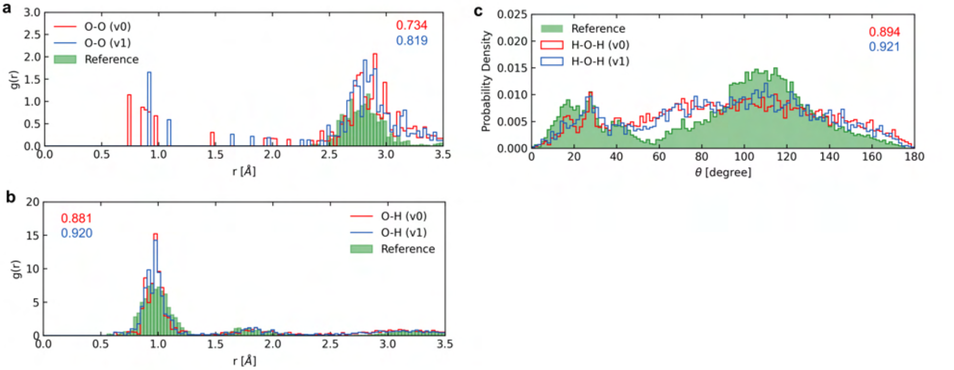

Prediction evaluations

Performance evaluation on **experimental AFM** images by comparing the **cosine similarity** $S(\mathbf{X}_0, \mathbf{X}_i) = \frac{\mathbf{X}_0 \cdot \mathbf{X}_i}{\|\mathbf{X}_0\| \|\mathbf{X}_i\|}$ between the properties $\mathbf{X}_i$ calculated from predicted structures and the reference values $\mathbf{X}_0$.

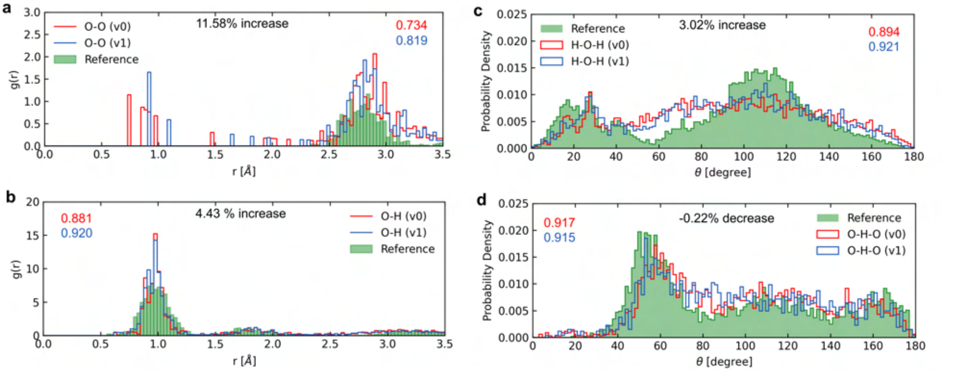

Discussion

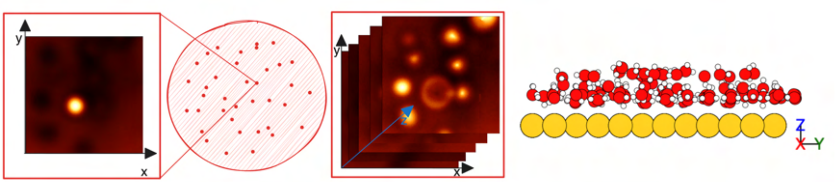

- We convert **3D AFM images to 2D** to train the style translation generator. This process can **disrupt the layer consistency**, potentially confusing the ML model when interpreting vertical information.

Discussion

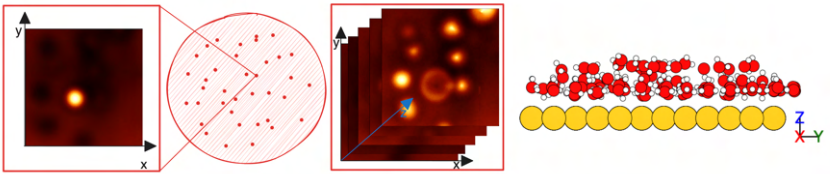

- We convert **3D AFM images to 2D** to train the style translation generator. This process can **disrupt the layer consistency**, potentially confusing the ML model when interpreting vertical information.
- The **resolution in the vertical (z) direction is much lower** than in the horizontal (x, y) plane, which complicates learning about AFM features in the vertical direction.

Discussion

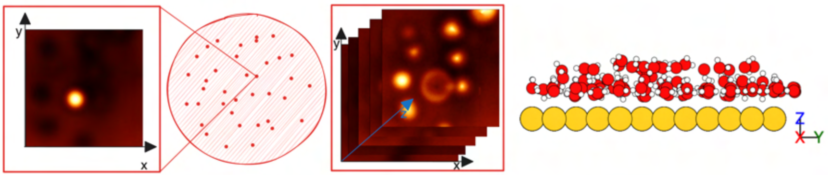

- We convert **3D AFM images to 2D** to train the style translation generator. This process can **disrupt the layer consistency**, potentially confusing the ML model when interpreting vertical information.
- The **resolution in the vertical (z) direction is much lower** than in the horizontal (x, y) plane, which complicates learning about AFM features in the vertical direction.
- Predicting 3D structures from AFM layers is challenging because the presence of all atoms affects the imaging of each layer. Layers of 2D AFM images cannot be viewed as **common 3D images** like computed tomography (CT) images, where **each layer is imaged independently**.

Discussion

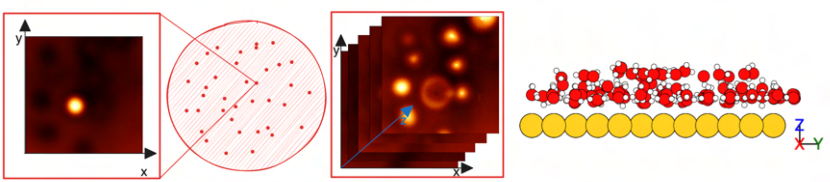

- We convert **3D AFM images to 2D** to train the style translation generator. This process can **disrupt the layer consistency**, potentially confusing the ML model when interpreting vertical information.
- The **resolution in the vertical (z) direction is much lower** than in the horizontal (x, y) plane, which complicates learning about AFM features in the vertical direction.
- Predicting 3D structures from AFM layers is challenging because the presence of all atoms affects the imaging of each layer. Layers of 2D AFM images cannot be viewed as **common 3D images** like computed tomography (CT) images, where **each layer is imaged independently**.
- The structure metrics we use are designed for systems of water molecules on gold surfaces.

Summary and future directions

- We applied CycleGAN to **translate styles between simulation** PPAFM **and real** AFM images.

Summary and future directions

- We applied CycleGAN to **translate styles between simulation** PPAFM **and real** AFM images.
- The trained generator shows the **ability to shift the PPAFM distribution towards the real** AFM distribution.

Summary and future directions

- We applied CycleGAN to **translate styles between simulation** PPAFM **and real** AFM images.
- The trained generator shows the **ability to shift the PPAFM distribution towards the real** AFM distribution.
- We developed **metrics to assess 3D structures** from AFM images, seeing **promising improvements** in most of these metrics. More properties like the number of hydrogen bond distribution will be included.

Summary and future directions

- We applied CycleGAN to **translate styles between simulation** PPAFM **and real** AFM images.
- The trained generator shows the **ability to shift the PPAFM distribution towards the real** AFM distribution.
- We developed **metrics to assess 3D structures** from AFM images, seeing **promising improvements** in most of these metrics. More properties like the number of hydrogen bond distribution will be included.
- We plan to use **more experimental images in CycleGAN training** to improve the style translation model.

Summary and future directions

- We applied CycleGAN to **translate styles between simulation** PPAFM **and real** AFM images.
- The trained generator shows the **ability to shift the PPAFM distribution towards the real** AFM distribution.
- We developed **metrics to assess 3D structures** from AFM images, seeing **promising improvements** in most of these metrics. More properties like the number of hydrogen bond distribution will be included.
- We plan to use **more experimental images in CycleGAN training** to improve the style translation model.
- We need to examine how the **hyper-parameters** like cycle consistency loss weight affect the results.

Acknowledgments

- Colleagues at the SIN group in Aalto University, Finland.
- Dr. Philipp Rahe's group, Universität Osnabrück, Germany.
- Prof. Ying Jiang's lab, Peking University, China.
- World Premier International Research Center Initiative (WPI), MEXT, Japan.
- The Academy of Finland (Projects 347319 and 346824).
- Computational resources provided by the Aalto Science-IT Project and CSC, Helsinki.